Development 140, 2443 (2013) doi:10.1242/dev.097626

Conserved and divergent functions of Nfix in skeletal muscle development during vertebrate evolution

Anna Pistocchi, Germano Gaudenzi, Efrem Foglia, Stefania Monteverde, Artal Moreno-Fortuny, Alessia Pianca, Giulio Cossu, Franco Cotelli and Graziella Messina

There was an error published in *Development* **140**, 1528-1536.

On p. 1532, the last line should state: the transcription of the NFATc4 isoform is dramatically increased after Nfix inhibition in murine fetal myoblasts (Messina et al., 2010).

The authors apologise to readers for this mistake.

Development 140, 1528-1536 (2013) doi:10.1242/dev.076315

Conserved and divergent functions of Nfix in skeletal muscle development during vertebrate evolution

Anna Pistocchi[1], Germano Gaudenzi[1], Efrem Foglia[1], Stefania Monteverde[1], Artal Moreno-Fortuny[1,2,*], Alessia Pianca[1], Giulio Cossu[1,3], Franco Cotelli[1] and Graziella Messina[1,‡]

SUMMARY

During mouse skeletal muscle development, the *Nfix* gene has a pivotal role in regulating fetal-specific transcription. Zebrafish and mice share related programs for muscle development, although zebrafish develops at a much faster rate. In fact, although mouse fetal muscle fibers form after 15 days of development, in fish secondary muscle fibers form by 48 hours post-fertilization in a process that until now has been poorly characterized mechanically. In this work, we studied the zebrafish ortholog *Nfix* (*nfixa*) and its role in the proper switch to the secondary myogenic wave. This allowed us to highlight evolutionarily conserved and divergent functions of Nfix. In fact, the knock down of *nfixa* in zebrafish blocks secondary myogenesis, as in mouse, but also alters primary slow muscle fiber formation. Moreover, whereas *Nfix* mutant mice are motile, *nfixa* knockdown zebrafish display impaired motility that probably depends upon disruption of the sarcoplasmic reticulum. We conclude that, during vertebrate evolution, the transcription factor Nfix lost some specific functions, probably as a consequence of the different environment in which teleosts and mammals develop.

KEY WORDS: Nfix, Skeletal myogenesis, Zebrafish, Slow muscle fibers, Sarcoplasmic reticulum

INTRODUCTION

Muscles are formed by subsequent myogenic waves, regulated by intrinsic and extrinsic signals during prenatal mammalian development (Biressi et al., 2007; Buckingham, 2007; Cossu and Biressi, 2005). The myotome is the first differentiated skeletal muscle, formed by mononucleated myocytes that differentiate in a Pax3/7-independent manner. All subsequent myogenic populations depend upon Pax3/7 expression (Gros et al., 2005; Hutcheson et al., 2009; Relaix et al., 2005). Embryonic myoblasts begin to fuse into primary multinucleated muscle fibers by E11, whereas fetal myoblasts fuse into secondary fibers between E14.5 and E17.5 (Cossu and Biressi, 2005). Once mature, skeletal muscles fibers differ in the expression of contractile protein isoforms and metabolic enzymes that confer a slow or fast twitching phenotype. Although zebrafish muscle development shares many features with amniotes, there are notable differences. The slow twitching fibers, derived from medial adaxial cells, are the first muscle fibers formed in zebrafish (Stickney et al., 2000). Adaxial originating cells are committed to a myogenic fate and express the myogenic regulator factors (MRFs) *myoD* and *myf5* (Coutelle et al., 2001; Weinberg et al., 1996). After somite formation, adaxial cells migrate radially from the notochord, form a layer of superficial slow fibers (SSFs) on the myotomal surface and express slow myosin heavy chain (MyHC) (Bryson-Richardson et al., 2005; Devoto et al., 1996; Du et al., 1997). After slow fiber precursor migration, fast fibers are specified in the deeper part of the somite and express fast MyHC (Blagden et al., 1997; Henry and Amacher, 2004; Stellabotte et al., 2007). At 24 hours post-fertilization (24 hpf), segmentation is complete and a functional myotome is formed. Following this primary myogenic wave in zebrafish, secondary slow twitching fibers differentiate in several body locations in a process called stratified hyperplasia or secondary myogenesis (48-72 hpf) (Devoto et al., 1996; Elworthy et al., 2008). In teleosts, muscle growth also occurs both by hypertrophy, owing to an increase in the size of pre-existing muscle fiber throughout life (Barresi et al., 2001), and hyperplasia, owing to the activity of Pax7-positive cells with typical muscle progenitor cell properties in the larval stage (Hollway et al., 2007; Seger et al., 2011).

Mouse embryonic and fetal myoblasts express distinct specific markers in the fibers they form (i.e. slow and fast MyHCs, MCK, β-enolase, PKCθ) (Biressi et al., 2007), indicating that embryonic and fetal myoblasts are intrinsically different populations of cells with distinct genetic programs. Among differentially expressed molecules, our group identified Nfix as a master switch regulator of the transcriptional transition from embryonic to fetal muscle (Messina et al., 2010).

Here, we report the identification of two zebrafish orthologs of Nfix, *nfixa* and *nfixb*, analyze their expression during development and use a loss-of-function approach to specifically abrogate the *nfixa* function *in vivo* and analyze the resulting muscle phenotype.

MATERIALS AND METHODS

Animals

Breeding wild-type fish of the AB strain were maintained at 28°C on a 14-hour light/10-hour dark cycle. Embryos were collected by natural spawning, staged according to Kimmel and colleagues (Kimmel et al., 1995) and raised at 28°C in fish water (Instant Ocean, 0.1% methylene blue) in Petri dishes, according to established techniques, approved by the veterinarian (OVSAC) and the animal use committee (IACUC) at the University of Oregon (USA), in agreement with local and national sanitary regulations. We express the embryonic ages in somites (s), hours post-fertilization (hpf) and days post fertilization (dpf). *MyoDCre* mice (Chen et al., 2005) and *Nfixc/+* mice, their genotyping strategies and manipulation have been already described (Campbell et al., 2008).

RT-PCR

Total RNA from 12 samples (an average of 30 embryos per sample) was extracted with the TOTALLY RNA isolation kit (Ambion), treated with

[1]Department of Biosciences, University of Milan, via Celoria 26, 20133 Milan, Italy. [2]Facultat de Biologia, Universitat de Barcelona, Diagonal 645, 08028 Barcelona, Spain. [3]Department of Cell and Developmental Biology, University College London, 21 University Street, London WC1E 6DE, UK.

*Present address: Department of Cell and Developmental Biology, University College London, 21 University Street, London WC1E 6DE, UK
‡Author for correspondence (graziella.messina@unimi.it)

Accepted 14 January 2013

RQ1 RNase-Free DNase (Promega) and oligo(dT)-reverse transcribed using SuperScript II RT (Invitrogen), according to manufacturers' instructions. PCR products were loaded and resolved onto 2% agarose gels.

The following primers were used: *nfixa*_sense, 5′-AGCGGTCAGAACAAACTGC-3′; *nfixa*_antisense, 5′-TCATTTAAATACGAGATCGATG-3′; *nfixb*_sense, 5′-CACCCTACGAGACGTGAGCA-3′; *nfixb*_antisense, 5′-GCCAGCTGCTCCTGACAATC-3′; *beta-actin*_sense, 5′-TGTTTTCCCCTCCATTGTTGG-3′; *beta-actin*_antisense, 5′-TTCTCCTTGATGTCACGGAC-3′; *fli1*_sense, 5′-AATATTGTCGGGCTCCACTG-3′; and *fli1*_antisense, 5′-CTTGGGTAAAGGAGCAGCAG-3′.

Primers for *myod* were used according to Amali and colleagues (Amali et al., 2004).

In situ hybridization, histological analysis, immunohistochemistry and transmission electron microscopy

Whole mount *in situ* hybridization experiments were carried out as described previously (Thisse et al., 1993). Immunohystochemistry and immunofluorescence analyses were carried out as described previously (Panzer et al., 2005). The following primers were used for PCR reactions to clone the probes: *nfixa* 300 bp_sense, 5′-AGCGGTCAGAACAAACTGC-3′; *nfixa* 300 bp_antisense, 5′-TCATTTAAATACGAGATCGATG-3′; *nfixb* 3′ UTR_sense, 5′-CACCCTACGAGACGTGAGCA-3′; *nfixb* 3′ UTR_antisense, 5′-GCCAGCTGCTCCTGACAATC-3′.

myod and *myog* probes were prepared has described previously (Schnapp et al., 2009). *smyhc1* probe has been kindly provided by the Ingham laboratory (Elworthy et al., 2008). Semi-thin histological sections were obtained as described previously (Cermenati et al., 2008). For transmission electron microscopy (TEM), thin sections were cut at 70 nm and placed onto copper grids, stained with 2% aqueous uranyl acetate and lead citrate, and analyzed under a Jeol 100 SX electron microscope. For immunohistochemistry and immunofluorescence in zebrafish, embryos were exposed to mouse anti-slow myosin heavy chain (F59, DSHB), mouse anti-sarcomeric (MF20, DSHB), mouse anti-ryanodin receptor (RyR:34C Sigma), mouse anti-*syt2b* (znp1, ZIRC), mouse anti-alcama (zn-5, ZIRC), mouse anti-sv2 (DSHB), mouse monoclonal anti-Pax7 (DSHB) and rabbit anti-*Nfix* (kindly provided by Richard Gronostajsky, State University of New York at Buffalo, USA), then treated with biotinylated or fluorescent secondary antibody (Vector Laboratories). Postsynaptic AChRs staining was performed as described previously (Panzer et al., 2005) (BTX, Molecular Probes, Eugene, OR). F59, MF20, H3P and Pax7 staining were performed as described previously (Devoto et al., 1996) and Seger and colleagues (Seger et al., 2011). Regarding the wild-type and skeletal muscle *Nfix*-null mice at E16.5/P3, immunofluorescence and transmission electron microscopy were carried out as described previously (Messina et al., 2010). Mouse anti-RyR was diluted 1:2000 and incubated for 1 hour at 37°C. Secondary antibodies used were Alexa Fluor 488 or 594-conjugated donkey anti-mouse. DAPI was used to stain the nuclei.

Quantitative real-time RT-PCR

Reverse transcriptions (RTs) were performed using 2 µg of DNase-treated (DNA-*free*, Ambion) total RNA in the presence of random hexamers (Invitrogen) and SuperScript II reverse transcriptase (Invitrogen). Real-time PCRs were carried out in a total volume of 15 µl containing 1× iQ SYBR Green Super Mix (BioRad), using 1 µl of the RT reaction. PCRs were performed using the BioRad iCycler iQ Real Time Detection System (BioRad Laboratories). For normalization purposes, *ef1a* RNA levels were tested in parallel with the gene of interest. The following primers were used: *nfixa*_sense, 5′-CCCCGTACTGCTTGACACA-3′; *nfixa*_antisense, 5′-GCTGTGGTTGGAGCACTGCGG-3′; *smyhc1*_sense, 5′-TGCCAAGACCATCAGAAATG-3′; *smyhc1*_antisense, 5′-CACACCAAAGTGAATTCGGATA-3′; *nfact4*_sense 5′-CAGGAGAAACCTCAGCTCAGTC-3′; *nfact4*_antisense, 5′-GGGTTCAATATCTCTTGAGGACA-3′; *ef1alpha*_sense, 5′-GGTACTTCTCAGGCTGACTGT-3′; and *ef1alpha*_antisense, 5′-CAGACTTGACCTCAGTGGTTA-3′.

Injections

To repress *nfixa* mRNA translation, an ATG-targeting morpholino (*nfixa*-MO) and an *nfixa*-splice-MO were synthesized (Gene Tools) (*nfixa*-MO, 5′-CCGGTCTCAAAGGCGGGAAATGATT-3′; *nfixa*-splice-MO, 5′-AAGAAAGAGAGTGTAACCCACTGAC-3′) and used at the concentration of 1 pmole in 1× Danieau buffer (pH 7.6) as previously reported (Nasevicius and Ekker, 2000). As a control, we injected a standard control morpholino oligonucleotide (ctrl-MO). The p53 morpholino has been designed (Gene Tools) and used as described previously (Robu et al., 2007).

The *in vivo* test of the specificity was carried out as described previously (Del Giacco et al., 2010). In brief, 300 pg/embryo of the pCS2+-*nfixa*-MO-GFP sensor plasmid have been injected alone or co-injected with 8 ng/embryo of *nfixa*-MO. The presence/absence of the GFP signal has been monitored under a fluorescent microscope from 24 to 48 hpf. *nfixa*-MO cDNA fragments inserted in the *Bam*HI site were obtained using the following complementary oligos: *nfixa*_MO sense, 5′-gatcAATCATTTCCCGCCTTTGAGACCGGCTAGCT- 3′; and *nfixa*_MO antisense, 5′-gatcAGCTAGCCGGTCTCAAAGGCGGGAAATGATT-3′.

For the specificity of phenotype, 8 ng of *nfixa*-MO were injected together with 200 pg/embryo of murine HA-*Nfix2* mRNA, 150 pg/embryo of *Mef2a*Flag mRNA and 150 pg/embryo *Mef2c*Flag mRNA, prepared as described previously (Biressi et al., 2007). The same results were obtained with the injection of 300 pg/embryo of the endogenous *nfixa* mRNA.

To repress *nfatc4* mRNA translation, an *nfatc4*-splice-MO was synthesized (Gene Tools) (*nfatc4*-splice-MO, 5′-CAGGAAAATGTGCTTCCCACCTGTA-3′) and used at the concentration of 8 ng/embryo. To validate *nfatc4*-splice-MO and verify the skipping of the second exon, following primers were used: *nfatc4*E1_sense: 5′-ACAGCAACCAGGAGTCTGC-3′; and *nfatc4*E3_antisense: 5′-ACGGTATGAATCCAGCAAGG-3′.

Sorting

Alpha-actin-GFP transgenic embryos (50-100) at 24 and 48 hpf were incubated in trypsin solution (0.5% trypsin and 1 mM EDTA) for 2 hours with gentle pipetting to dissociate the cells. Cells were resuspended in PBS (Gibco)/20% fetal calf serum (FCS; BioWhittaker)/20 mM HEPES and 2 mM EDTA and filtered through 40 µm cell strainers (Falcon) before sorting using a Vantage Sorter SE (Becton Dickinson) at a flow rate of 3000 cells per second. GFP was exited at 488 nm using an argon laser. Cells dissociated from wild-type embryos were used to set the gating to exclude green autofluorescence. After sorting, the *GFP*+ cells were collected and RNA was extracted with the micro-RNAeasy kit (Qiagen). RNA was directly retro-transcribed with the iSCRIPTtm cDNA synthesis kit (BioRad) and the obtained cDNA was used for RT-PCR reactions.

Western blot

Fish embryos and mouse fetuses were lysed in RIPA buffer (5 µl for each zebrafish embryo) and homogenized. Samples were boiled for 10 minutes at 95°C. Zebrafish protein samples (20 µl) were size-fractionated by gel Pre-cast (Invitrogen) and transferred with iBlot (Invitrogen). The nitrocellulose membranes were blocked with 5% non-fat dry milk in PBST (PBS containing 0.1% Tween 20) for 30 minutes at room temperature and subsequently incubated with the primary antibody: mouse anti-slow myosin heavy chain (F59, DSHB), mouse anti-sarcomeric myosin (MF20, DSHB), rabbit anti-Nfix and mouse anti-β-tubulin (Covance), mouse anti-RyR:34C (Sigma), mouse monoclonal anti-Pax7 (DSHB) diluted in 5% milk/PBST overnight at 4°C. Horseradish peroxidase-conjugated secondary antibody (BioRad) were used for 30 minutes at room temperature. The antigen signal was detected with the ECL chemiluminescence detection system (Amersham), as specified by the manufacturer.

Cyclosporine (CsA) treatment

Controls and *nfixa*-MO-injected embryos were dechorionated at shield or at 8-10 somite stage and incubated in CsA for 12 hpf. CsA was used at 100 mM and dissolved in 0.1% DMSO in egg water. Vehicle control treatment consisted of 0.1% DMSO in egg water.

RESULTS

Identification of zebrafish nfixa and nfixb genes

As a first step, we sought to identify the ortholog(s) of Nfix in zebrafish. Ensembl search using human Nfix as a bait, identified two candidates referred to as *nfixa* gene (assembly Zv9,

chromosome 1, nucleotide position 52,397,904-52,595,159) and *nfixb* (assembly Zv9, chromosome 3, nucleotide position 14,397,904-14,663,156). Analysis of the amino acid sequence homology between human, murine and the two zebrafish Nfix orthologs revealed high degree of conservation among them but did not reveal which zebrafish gene was the functional ortholog (supplementary material Table S1). Analysis of *nfixa* and *nfixb* chromosomal organization (Fig. 1A), and phylogenetic tree (Fig. 1B) of the NfI family across vertebrates revealed that both genes are co-orthologs of the mammalian Nfix and they could arise from a recent fish lineage-specific duplication event (Taylor et al., 2003).

RT-PCR analyses of *nfixa* and *nfixb* showed expression of both transcripts in the developing embryo, larva and in adult muscle (Fig. 1C). Therefore, to determine whether one or both orthologs are expressed during muscle formation, we examined the spatial and temporal distribution of *nfixa* and *nfixb* transcripts by whole-mount *in situ* hybridization. The *nfixa*-specific probe (*nfixa*) revealed a hybridization signal in the notochord, in the unsegmented paraxial mesoderm at the 5-somite stage (Fig. 1D) and in the segmented mesoderm at 8- to 10-somite stage (Fig. 1D′). By contrast, we did not detect any specific labeling for *nfixb* in already formed somites (supplementary material Fig. S1A). We also noted that by 3 days post-fertilization (3 dpf) the labeling of both *nfixb*

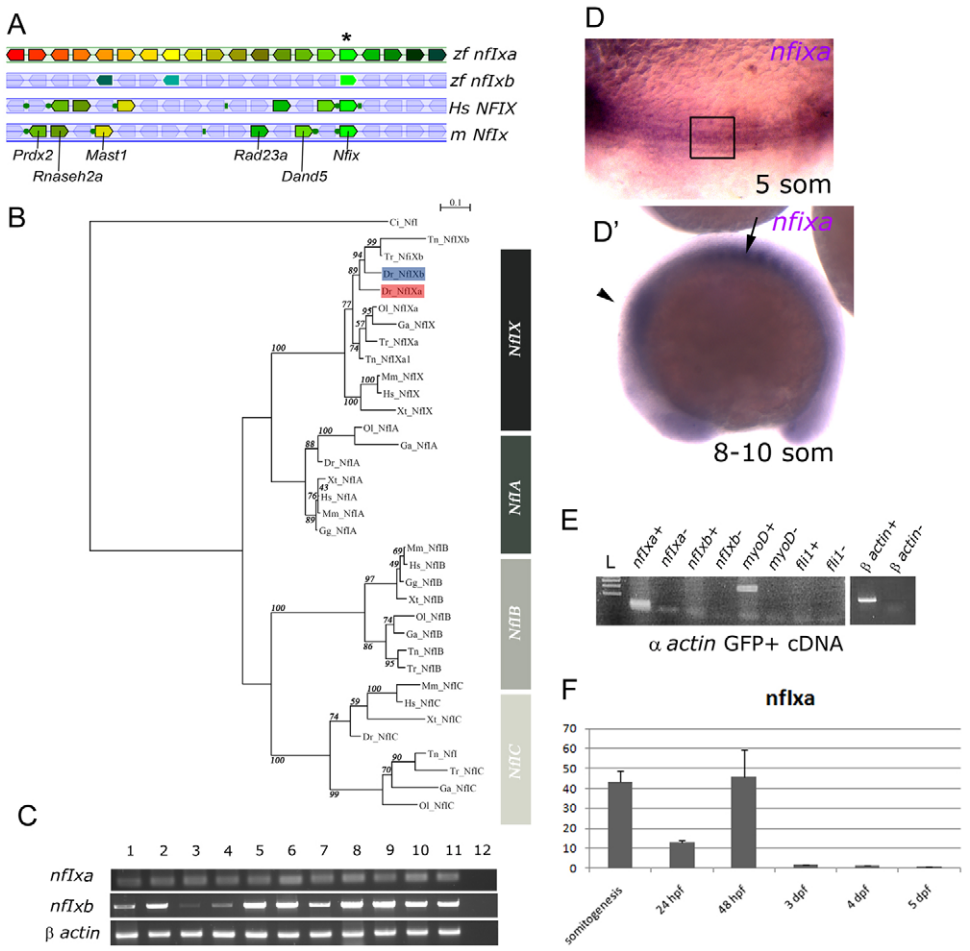

Fig. 1. Identification and expression analysis of *nfixa* and *nfixb*. (**A**) Each zebrafish *nfix* gene is shown as a reference locus. Genes annotated as paralogs (no surrounding line) or orthologs (with a surrounding line) by the Ensembl database share the same color; blue lines beneath individual tracks indicate that orientations of gene blocks and are inverted with respect to their genomic annotation. Analysis of chromosomal organization for zebrafish *nfixa* (chromosome 1), *nfixb* (chromosome 3), and the human (chromosome 19) and mouse (chromosome 8) Nfix genes. Syntenous human and mouse genes are labeled. The figure was derived from the output of the Genomicus website (version 57.01). (**B**) Phylogenetic relationship of Nfi genes. Evolutionary comparison of different members of Nfi protein family represented in a Maximum-likelihood bootstrap consensus tree. The zebrafish *nfixa* and *nfixb* are highlighted. Branch lengths are measured in terms of amino acid substitutions, with the scale indicated over the tree. Numbers at nodes indicate percent of bootstrap probabilities. Ce, *Caenorhabditis elegans*; Ci, *Ciona intestinalis*; Dr, *Danio rerio*; Ga, *Gasterosteus aculeatus*; Gg, *Gallus gallus*; Hs, *Homo sapiens*; Mm, *Mus musculus*; Ol, *Oryzias latipes*; Tn, *Tetraodon nigroviridis*; Tr, *Takifugu rubripes*; Xt, *Xenopus tropicalis*. (**C**) RT-PCR performed at different developmental stages: ladder (L), one- to two-cell stage (lane 1), 30% epiboly (lane 2), 50% epiboly (lane 3), tail bud (lane 4), eight somites (lane 5), 15 somites (lane 6), 24 hpf (lane 7), 48 hpf (lane 8), 3 dpf (lane 9), 5 dpf (lane 10), adult muscle (lane 11) and negative control (lane 12) in the absence of cDNA. (D,D′) Whole-mount in situ hybridization with *nfixa*-specific probe at the 5-somite stage and 8-10 somite stage. (**D**) The transcript is present in the unsegmented paraxial mesoderm and in the notochord (boxed region). (**D′**) *nfixa* signal is present in the already segmented somites (arrow) and in the central nervous system (arrowhead). (**E**) RT-PCR performed on cDNA of muscle cells sorted from α-actin GFP transgenic embryos at 24 and 48 hpf. White line marks lanes run on a separate gel but using the same samples and amounts of input RNA. (**F**) Quantitative real-time PCR (qRT-PCR) of *nfixa* mRNA expression normalized to *ef1a*.

and *nfixa* probes is restricted to the telencephalon and mesencephalon (supplementary material Fig. S1B,C). To further analyze *nfixa* and *nfixb* expression specifically in muscles, we FACS sorted muscle cells from α-actin transgenic embryos at 24 and 48 hpf. cDNA from sorted cells was analyzed by RT-PCR and, as shown in Fig. 1E, only *nfixa* is expressed in muscle cells. *myod* was used as a positive control for the enrichment of muscle cells, whereas the vascular marker *fli1* was used as a negative control (Thompson et al., 1998). On the basis of these results, we focused our study on *nfixa*. Expression of *nfixa* was therefore quantified by qRT-PCR on cDNA obtained exclusively from tails (to exclude expression in the CNS) (Fig. 1F). *nfixa* expression is high during somitogenesis and at 48 hpf, but lower at 24 hpf and close to background after 48 hpf. Interestingly, this expression pattern correlates with the first and second myogenic waves that occur during somitogenesis and from 48 hpf (Barresi et al., 2001; Stellabotte et al., 2007).

Nfixa loss of function in zebrafish leads to muscle disorganization and impairs fish motility

To achieve insight into the role of *nfix* during zebrafish muscle development, we specifically knocked down the *nfixa* gene by injecting an antisense oligonucleotide morpholino (MO, Gene Tools) designed against the start site of the *nfixa* transcript (*nfixa*-MO). In all experiments, *nfixa*-MO-injected embryos were compared with embryos injected with the same amount of a non-specific control MO (ctrl-MO) at the same developmental stage.

To test the *in vivo* efficiency of *nfixa*-MO, the *nfixa*-GFP sensor plasmid was co-injected with *nfixa*-MO or ctrl-MO, respectively (Fig. 2). The presence/absence of the GFP was monitored under a fluorescent microscope from 24 to 48 hpf. Most (90% *n*=30) of the embryos injected with the sensor plasmid alone were positive for the GFP (Fig. 2A,A′). This percentage decreased to 25% (*n*=80) when the plasmid was co-injected with *nfixa*-MO, indicating that *nfixa*-MO specifically binds to its target region (Fig. 2B,B′). Notably, embryos injected with a splice-morpholino designed to exon 2-intron 2 junction (*nfixa*-MO2, 1 pmol/embryo), showed the same phenotype as the *nfixa*-MO. Nfix protein reduction in embryos injected with both AUG-*nfixa*-MO and splice-site *nfixa*-MO2 was also confirmed by western blot analysis (Fig. 2C,C′). Therefore, for all the following results, we used indistinguishably *nfixa*-MO or *nfixa*-MO2, and referred to both as *nfixa*-MO.

We observed that, up to 3 dpf, *nfixa*-MO-injected embryos showed normal somite number and size, as well as normal muscle formation and movements (data not shown). Moreover, *nfixa* knockdown did not affect any of the myogenic markers examined (*myod* and *myog*), suggesting that the segmentation process and the first myogenic wave take place properly (supplementary material Fig. S2). However, from 3 dpf, the majority of *nfixa*-MO-injected embryos (80%, *n*=150) appeared partially or completely immotile, failed to hatch from their chorion and to respond to external stimuli (touch response defects) (see supplementary material Movies 1, 2). All the *nfixa*-MO injected embryos died at 6 dpf.

To exclude that motility impairment could be due to motoneuron defects, we sorted *islet1*-positive motoneurons from the transgenic line *islet1*-GFP (Higashijima et al., 2000) and verified by RT-PCR that *nfixa* is not expressed in motoneurons (supplementary material Fig. S3A). Moreover, *islet1* expression was not changed at 48 hpf (supplementary material Fig. S3B,B′) and axonal projections of primary and secondary motoneurons (visualized by znp1 and zn-5 antibodies, respectively) were correctly formed in *nfixa*-MO-injected embryos at 3 dpf (supplementary material Fig. S3C-D′).

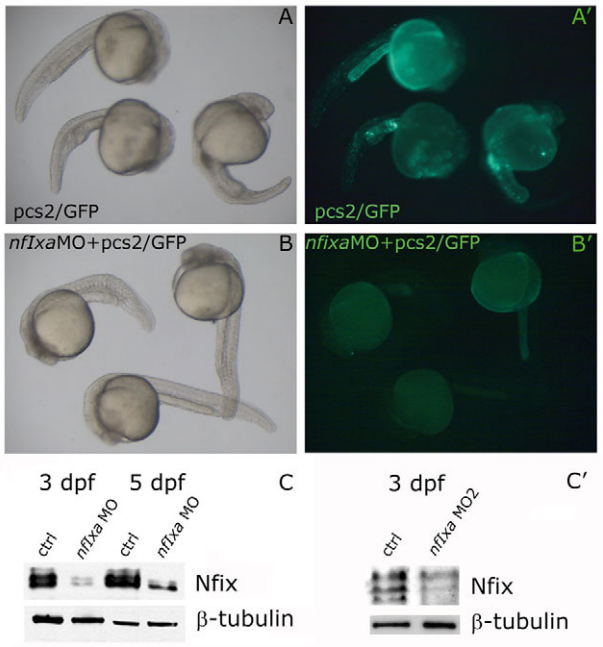

Fig. 2. *nfixa*-MO specifically reduces *nfixa*-GFP sensor mRNA translation and Nfi protein levels. For the *in vivo* test of the specificity of *nfixa*-MO, an *nfixa*-GFP sensor has been generated. The pCS2+ construct containing the sequence recognized by the *nfixa*-MO fused with the GFP open reading frame was used for injection experiments with ctrl-MO or with the *nfixa*-MO. (**A**,**A′**) Embryos at 24 hpf: GFP-positive cells in the trunk and in the yolk epithelium following co-injection of the sensor and the control-MO. (**B**,**B′**) The complete absence of GFP expression when the sensor is co-injected with *nfixa*-MO confirms the specificity of the morpholino action. In A,A′, embryos are visualized under normal light; in B,B′ embryos are under fluorescent light. (**C**,**C′**) The morpholino efficiency has also been tested by means of western blot experiments; Nfix protein levels are decreased both in AUG-*nfixa*-MO (C) and splice-*nfixa*-MO2 (C′) injected embryos in comparison with control embryos at the same developmental stages.

Moreover, to analyze neuromuscular junctions, we labeled acetylcholine receptor synapses with bungarotoxin (BTX, postsynaptic AChRs) and synaptic vesicle 2 with anti-SV2 (presynaptic vesicles) antibodies (Panzer et al., 2005). The co-staining of both signals in control and *nfixa*-MO injected embryos at 3 dpf showed mature neuromuscular synapses (supplementary material Fig. S3E-F″), thus providing evidence that the phenotype observed in the *nfixa*-MO injected embryos is specifically due to muscular defects.

It is known that morpholino molecules could elicit undesirable off-target effects such as activation of the p53 protein (Robu et al., 2007). Therefore, as an additional control we performed the co-injection of the *nfixa*- and the *p53*-MO that did not recover the defects in motility, sarcoplasmic reticulum development and the slow MyHC levels at 3 dpf, indicating that possible p53 activation is not responsible for the muscle defects due to *nfixa* loss of function (data not shown).

To further validate a cause-effect relationship between lack of *nfixa* and the subsequent phenotype in the *nfixa*-MO-injected embryos, we performed phenotypic/functional rescue experiments. We have previously described that, in mouse, Mef proteins participate in Nfix activity (Messina et al., 2010). Therefore, to rescue the *nfixa*-MO phenotype we co-injected mouse *Nfix2* (one of the splicing isoforms of *Nfix*), together with its co-factors *Mef2a*

and *Mef2c* mRNAs (Messina et al., 2010). We observed that only the co-injection of *Nfix2* with *Mef2a*/*Mef2c* rescues the immotile phenotype in 35% of the injected embryos (n=70), whereas the injection of the single *Nfix2* transcript did not, recapitulating the murine mechanism (see supplementary material Movie 3). A rescue of the phenotype was also obtained by injecting the zebrafish *nfixa* mRNA (data not shown).

To obtain a detailed insight of the immotile phenotype, we made histological semi-thin sections of control and *nfixa*-MO-injected embryos but no evident morphological changes were observed at 48 hpf (data not shown). However, sections from 3 dpf *nfixa*-MO-injected embryos showed disorganized, centrally nucleated fibers, which are characteristic of an immature hypertrophic state (Fig. 3A,B). In addition, myofibers of 3 dpf *nfixa*-MO-injected embryos appeared less dense than control in transmission electron microscopy (TEM): in a given area of 0.4 μm^2, 46±5 fibers were present in control and only 24±4 fibers in *nfixa*-MO (n=10 different fields scored in three different control and treated embryos, Fig. 3D,E). Notably, fibers of *nfixa*-MO injected embryos showed an extremely reduced, close to absent, sarcoplasmic reticulum (SR) between the sarcomeres (Fig. 3G,H), thus explaining the impairment to move and swim. As specific marker of SR, we looked at the levels of the calcium-channel ryanodin receptors (RyRs) in control and *nfixa*-MO-injected embryos. Immunofluorescence (Fig. 3J-K) and western blot analyses (Fig. 3M) showed a strong inhibition of RyRs following *nfixa* loss of function. In addition, in *Nfix2-Mef2a/Mef2c* rescued embryos, fiber organization and the levels of RyRs were partially recovered (Fig. 3C,F,I,L,M). The absence of SR was not documented before in the muscle-specific skeletal muscle *Nfix*-null mouse (Messina et al., 2010). For this reason, we investigated more thoroughly the SR phenotype both in mouse fetal E16.5 and in postnatal P3 developmental stages. In mouse, the SR is present (supplementary material Fig. S4A-D) and levels of RyRs are comparable between wild-type and *Nfix*-null E16.5 fetuses and postnatal P3 mice (supplementary material Fig. S4C-E″). Therefore, the absence of the SR appears as a specific feature for zebrafish *nfixa* loss-of-function.

In the absence of *nfixa*, primary slow MyHC levels remain elevated and the second myogenic wave is impaired

We have previously demonstrated that mis-expression of Nfix in mouse causes an altered expression of slow MyHC: both transcript and protein levels decrease when *Nfix* is overexpressed, while the increase when *Nfix* is inhibited (Messina et al., 2010).

As in zebrafish *smyhc1* is a marker of primary slow fibers (Elworthy et al., 2008; Henry and Amacher, 2004), we compared its expression during development in control and *nfixa*-MO injected fish. By qRT-PCR and whole-mount *in situ* hybridization analyses, we observed that in controls the physiological expression of *smyhc1* peaks at 48 hpf, at the onset of the second myogenic wave, and decreases after 48 hpf. By contrast, the level of *smyhc1* in *nfixa*-MO injected embryos remains elevated even after 48 hpf (Fig. 4A-C). Moreover, by using F59 antibody (which recognizes the primary slow fibers (Devoto et al., 1996), we observed that not only the transcript of primary slow myosin, but also slow MyHC protein levels are still high in the *nfixa*-MO-injected embryos (Fig. 4D-F). Interestingly, in rescued larvae the levels of F59 slow myosin decreases to levels comparable with control siblings (Fig. 4D). To confirm that this effect is specific for slow myosin and is not dependent on a developmental delay after *nfixa* loss of function, we checked that vessel formation was comparable in control and *nfixa*-MO *fliI*-GFP transgenic injected embryos (Thompson et al., 1998). As shown in supplementary material Fig. S5, even though the morphology of *nfixa* morphants is altered, the vascular tree is correctly formed and does not show developmental delay.

It has previously been demonstrated that NFAT family members regulate the transcription of slow MyHC in adult muscle (Calabria et al., 2009) and that the transcription of the NFATc4 isoform is dramatically decreased after Nfix inhibition in murine fetal

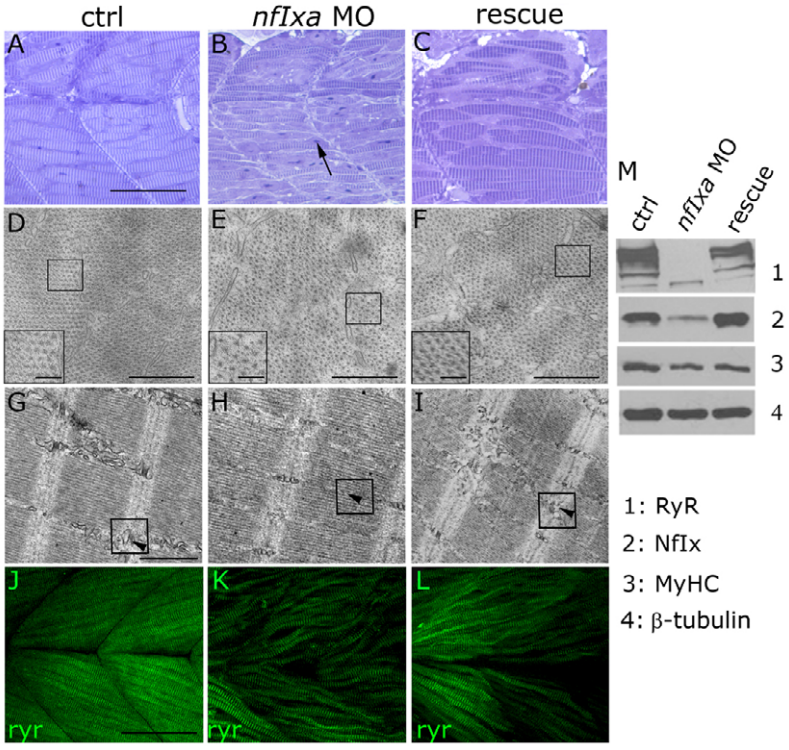

Fig. 3. *Nfixa* loss-of-function effects become evident from 48 hpf. (**A-C**) At 3 dpf, muscle fibers in *nfixa*-MO-injected embryos are disorganized and present rounded, dark stained nuclei in comparison with control embryos (arrow). (A-C) Longitudinal semi-thin sections. (**D-I**) Electron microscopy of 3 dpf control and *nfixa*-MO-injected embryos. (D-F) Transverse and (G-I) longitudinal sections. The sarcomeric structure in *nfixa*-MO-injected embryos is less dense but correctly organized (E) in comparison with controls (D). Sarcomeric reticulum (arrowheads in G,H) is absent in *nfixa*-MO-injected embryos (H). Boxes in D-F correspond to higher magnifications of the same picture. (**J-M**) Immunofluorescence (J-L) and western blot (M) experiments demonstrate that RyR levels are decreased in *nfixa*-MO-injected embryos at 3 and 5 dpf in comparison with control embryos at the same developmental stages and return to normal levels in rescued embryos. (C,F,I,L) The phenotype was partially rescued by the injection of the murine *Nfix2* transcript with its co-factors *Mef2a/Mef2c*. Scale bars: 10 μm in A-C,J-L; 0.5 μm in main image, 0.1 μm in insets in D-F; 0.5 μm in G-I.

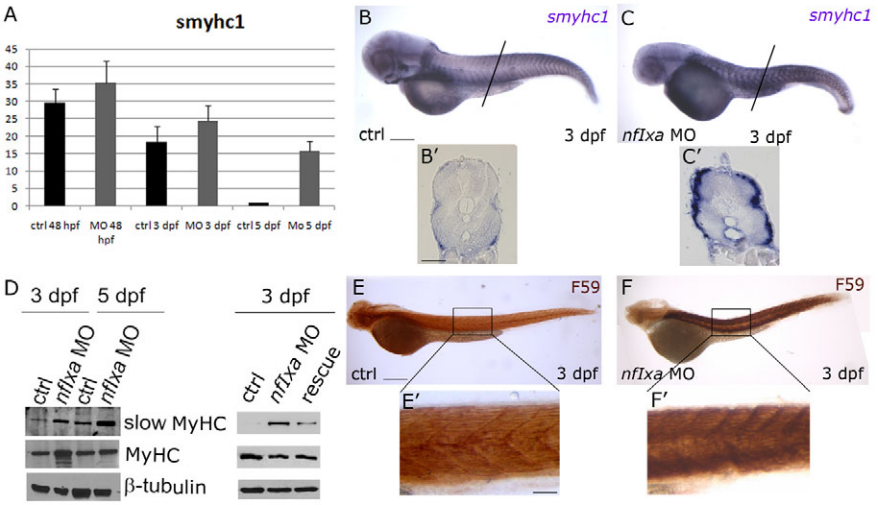

Fig. 4. Slow myosin remains expressed in *nfixa*-MO injected embryos after 48 hpf. (**A**) Quantitative real-time PCR (qRT-PCR) of *smyhc1* mRNA expression normalized to *ef1a*. The expression of *smyhc1* in control embryos presents a peak at 48 hpf and is then downregulated at 3 and 5 dpf. In *nfixa*-MO-injected embryos, the expression of *smyhc1* remains elevated even after 48 hpf. (**B-C′**) Whole-mount *in situ* hybridization with *smyhc1* probe replicates qRT-PCR results: at 3 dpf, *nfixa*-MO-injected embryos (C,C′) still present a stronger signal of *smyhc1* than controls (B,B′). B′ and C′ are transverse sections of the tail. (**D**) Western blot: slow myosins are recognized by F59 antibody; all sarcomeric myosins are recognized by MF20 antibody. At 3 and 5 dpf in *nfixa*-MO injected embryos, slow and all myosin protein levels are higher than the control, whereas protein levels were recovered in rescued embryos at 3 dpf. Additional lower molecular weight bands in the 3 dpf *nfixa*-MO MyHC lane correspond to degradation products of the protein. (**E-F′**) Immunostaining with F59 antibody (slow fibers): at 3 dpf, *nfixa*-MO-injected embryos (F,F′) present a stronger F59 signal than the control (E,E′). Insets in E′ and F′ show a higher magnification of the tail region. In all figures, lateral views are shown, anterior is always towards the left. Scale bars: 100 µm in B,B′,C,C′,E,F; 200 µm in E′,F′.

myoblasts (Messina et al., 2010). The *nfatc4* ortholog is present in zebrafish (ENSDARG00000054162 chromosome 2: 37,496,488-37,524,447), and, by qRT-PCR, we verified that its level decreased during the second myogenic waves, suggesting a possible *nfatc4*-mediated regulation of primary slow MyHC in fish as well as in amniotes (Fig. 5A). We therefore tested whether *nfixa* could repress slow MyHC expression by inhibiting the transcription of *nfatc4*; as shown in Fig. 5A, the level of *nfatc4* remains elevated in *nfixa*-MO injected embryos.

To confirm that *nfatc4* is negatively regulated by *nfixa* and that, in the absence of *nfixa*, *nfatc4* allows the persistent expression of genes involved in primary slow fiber differentiation, we designed a splice-*nfatc4*-MO to inactivate zebrafish *nfatc4* function. We validate the splice-*nfatc4*-MO by RT-PCR, showing the skipping of the second exon (150 bp) in the *nfatc4*-MO injected embryos at 24 hpf. RT-PCR primers were designed in exon 1 and exon 3, respectively; the amplification product, that includes the second exon, was 326 bp in control embryos, whereas two bands at 326 bp and 174 bp, respectively, were detected in splice-*nfatc4*-MO injected embryos, confirming the partial skipping of the second exon (Fig. 5B).

We co-injected the *nfixa* and the *nfatc4* morpholinos and observed a reduction of the primary slow fibers by F59 immunohistochemistry

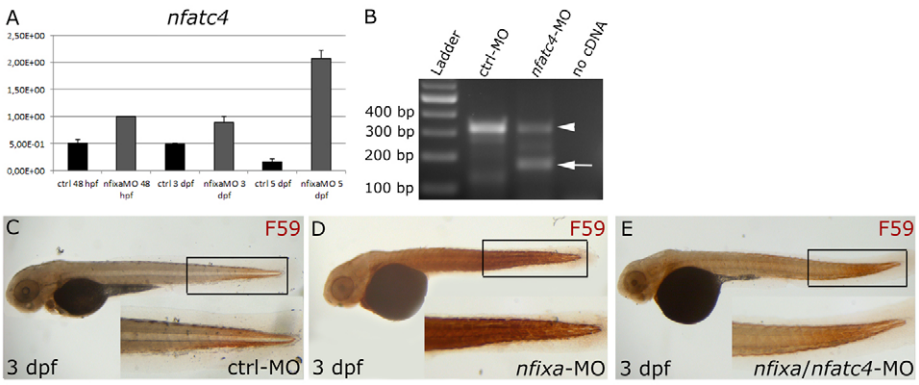

Fig. 5. Evolutionarily conserved inhibition of *nfatc4* by *nfixa* and regulation of primary slow fibers. (**A**) Quantitative real-time PCR (qRT-PCR) of *nfatc4* mRNA expression normalized to *ef1a*. The expression of *nfatc4* remains elevated in 48 hpf, 3 and 5 dpf *nfixa*-MO injected embryos, compared with controls. (**B**) RT-PCR on control and splice-*nfatc4*-MO-injected embryos at 24 hpf. RT-PCR primers were designed in exon 1 and exon 3, respectively; the amplification product, which contains the second exon, was 326 bp in control embryos, whereas two bands at 326 bp (arrowhead) and 174 bp (arrow) were detected in splice-*nfatc4*-MO injected embryos, confirming the partial skipping of the second exon (150 bp). (**C-E**) Immunostaining with F59 antibody (slow fibers): at 3 dpf, *nfixa-nfatc4*-MO injected embryos (E) present a F59 signal comparable with controls (C), whereas F59 remains elevated in *nfixa*-MO-injected embryos (D).

(Fig. 5C-E). Similar results were obtained by blocking *Calcineurin/Nfatc4* signaling with cyclosporine A (CsA) treatment (Chang and Mun, 2004) in *nfixa*-MO-injected embryos (data not shown).

These data unequivocally demonstrate an evolutionarily conserved role of *nfixa* in primary slow fiber regulation through a mechanism that involved the Mef2a-Mef2c machinery and that negatively regulated the *nfatc4* expression.

The *Nfix*-deficient mouse presents a block in fetal myogenesis that leads to a persistence of slow embryonic fibers. We therefore wondered whether, as in mammals, new secondary fiber development does not occur in fish because primary slow MyHc fibers remain predominant. First, we analyzed the rate of proliferation in muscles at 3 dpf: in comparison with control (Fig. 6A), *nfixa*-MO-injected larvae presented an increased number of proliferating H3P muscle cells (Fig. 6B), whereas rescued larvae presented a number of H3P-positive cells that was comparable with controls (Fig. 6C). Then, to check specifically secondary fiber formation, we looked at the dorsal and ventral extremities of the superficial muscle monolayer, as described by Barresi and colleagues (Barresi et al., 2001). As clearly shown by histological semi-thin sections (Fig. 6D,E) and also confirmed by TEM analysis (data not shown) and by confocal images of all sarcomeric MyHCs expression (Fig. 6G-I), these secondary fibers do not form in *nfixa*-MO-injected embryos at 3 dpf, whereas they are present in rescued embryos. Moreover, we injected embryos with *nfixa*-MO and treated them with cyclopamine, which inhibits Hh signaling and blocks primary slow fiber formation (Biressi et al., 2008; Chen et al., 2002). Cyclopamine-treated control embryos normally developed secondary slow muscle fibers at the dorsal and ventral extremes of the myotome, whereas in *nfixa*-MO-injected embryos the secondary fibers were not formed. This phenotype was partially rescued by the injection of the murine *Nfix2* transcript (Fig. 6J-L). Several lines of evidence present Pax7 as an expression marker of muscle progenitor cells that generate fibers during a secondary period of zebrafish larval muscle growth (Hollway et al., 2007; Seger et al., 2011). We thus investigated whether in *nfixa*-MO-injected embryos secondary fibers do not form owing to the absence of pax7-positive-progenitor cells. Immunofluorescence (Fig. 7A-F) and western blot analyses (Fig. 7G) performed on protein extracted

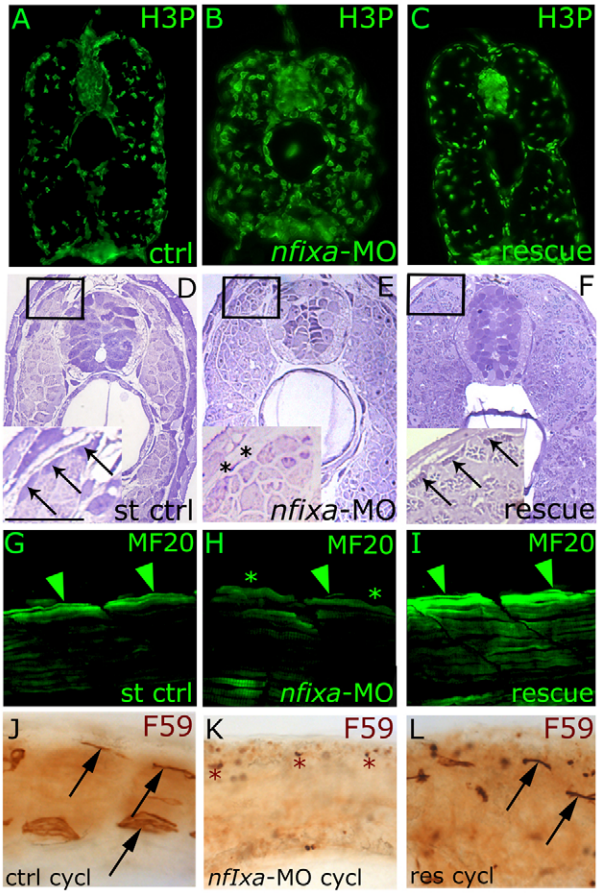

Fig. 6. Secondary slow fibers do not form in *nfixa*-MO-injected embryos. (**A-C**) Immunohistochemistry experiments with the H3P antibody that recognizes proliferating cells. *nfixa*-MO-injected larvae (B) presented an increased rating of proliferation at 3 dpf in comparison with controls (A) and rescued larvae (C). (**D-I**) Secondary fibers at the dorsal and ventral extremes of the superficial muscle monolayer did not form in 3 dpf *nfixa*-MO-injected embryos (E,H, asterisks) in comparison with controls (D,G, arrows and arrowheads), whereas they are recovered in rescued embryos (F,I, arrows and arrowheads). (D-F) Histological semi-thin sections, inset shows higher magnification. (G-I) Confocal images of MF20 immunostaining. (**J**,**K**) Lateral views of F59 labeling, which is maintained in the extreme dorsal and ventral regions of embryos treated with cyclopamine (arrows) but absent in *nfixa*-MO-injected embryos (K, asterisks). (**L**) In rescued embryos treated with cyclopamine, the formation of secondary fibers is partially recovered in small areas (arrows). (A-F) Transverse sections, dorsal on top. (G-L) Lateral views, anterior is always towards the left. Scale bar: 100 μm.

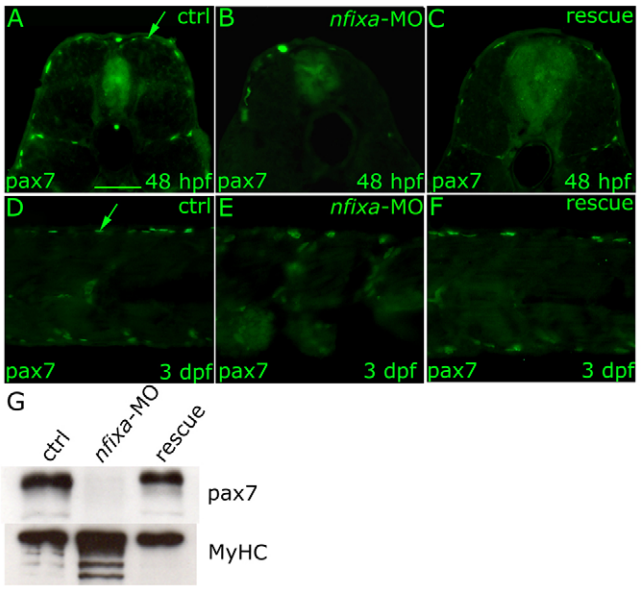

Fig. 7. The absence of Pax7-positive progenitor cells in *nfixa*-MO-injected embryos determines the loss of secondary fibers. (**A-F**) Immunohistochemistry experiments with the Pax7 antibody that recognizes secondary fiber precursors. Pax7-positive secondary fiber progenitors at the dorsal and ventral extremes of the superficial muscle monolayer did not form in 48 hpf and 3 dpf *nfixa*-MO-injected embryos (B,E) in comparison with controls (A,D arrow), whereas they are recovered in rescued embryos (C,F). (**G**) Western blot: secondary fiber precursors were recognized by Pax7 antibody, all sarcomeric myosins MyHC were recognized by MF20 antibody. In isolated tails of *nfixa*-MO-injected larvae, Pax7 protein levels were higher than the control whereas they were recovered in rescued embryos at 3 dpf. All myosin protein levels were higher in *nfixa*-MO-injected larvae, as expected. (A-C) 48 hpf transversal sections, dorsal on top. (D-F) 3 dpf longitudinal sections, anterior towards the left. Scale bar: 100 μm.

from the tails (to exclude the CNS component) showed a strong downregulation of Pax7 following *nfixa* loss of function at 3 dpf. In addition, in rescued embryos, Pax7-positive secondary progenitors fibers in the lateral surface of the myotome and Pax7 protein levels in the trunk were partially recovered (Fig. 7A-F).

Together, these data show the existence of a functional conservation of the role of *nfixa* in the regulation of the second myogenic wave: its absence determines persistent expression of primary slow fibers and prevents the switch towards the second myogenic wave owing to the absence of the Pax7-positive precursor cells.

DISCUSSION

The four nuclear factor one (NFI) genes *Nfia*, *Nfib*, *Nfic* and *Nfix* are highly conserved in vertebrates and are expressed in different tissues both in the embryo and in the adult. In mouse, specific knockdown of each gene demonstrated their essential role for the proper development of the embryo (Nasevicius and Ekker, 2000; Steele-Perkins et al., 2003; Steele-Perkins et al., 2005). In particular, the *Nfix* gene is involved in the development of brain, spinal cord and skeletal muscle, in which it regulates the transition from embryonic to fetal gene expression, a role with a profound evolutionary significance in amniotes (Campbell et al., 2008; Driller et al., 2007; Messina et al., 2010). Fetuses that lack *Nfix* in skeletal muscle are smaller and have fibers with a reduced diameter, whereas embryos prematurely expressing the isoform *Nfix2* are larger, reflecting more robust transcription of fetal muscle genes (Messina et al., 2010). In particular, we demonstrated that Nfix represses the expression of slow myosin heavy chains, which are responsible for slow twitching contractile activity. Although the mechanisms that regulate the secondary fiber formation in zebrafish have been poorly characterized until now, our data shed light on conserved and divergent function of Nfix in this process, leading to the hypothesis of the conserved role for this gene may reflect the existence of a parallelism between the two myogenic waves in zebrafish and mouse.

In zebrafish, there are two ortholog of Nfix that we named *nfixa* and *nfixb*; however, only *nfixa* is expressed in embryonic muscles. The loss-of-function approach led us to identify a defined role for *nfixa* during muscle development. Until 48 hpf, *nfixa* loss-of-function embryos are indistinguishable from control siblings and proper expression of myoblast-specific transcription factors *myod* and *myog* confirms that commitment and myogenic differentiation of somitic cells is not affected. However, after 48 hpf, embryos show reduced motility and larvae do not survive to adulthood. These phenotypes are consistent with defects in skeletal muscle, as already shown in several mutants with reduced touch response or motility (Granato et al., 1996). Indeed, when *nfixa* is downregulated, muscle structure is altered and not properly organized, as in the *Nfix*-null fetus (Messina et al., 2010). As *nfixa* is also expressed in the CNS by 3 days post-fertilization, we verified that motoneurons, their axonal projections and neuromuscular junctions were correctly formed in *nfixa*-MO-injected embryos, excluding any defects resulting from to alterations in motoneuron development.

To our surprise, the sarcoplasmic reticulum is reduced or absent in *nfixa*-MO-injected zebrafish embryos, thus explaining defects of contraction and motility. This Nfix function appears not to be conserved between fish and mammals, as in the fetus and newborn (P3) skeletal muscle *Nfix*-null mice the sarcoplasmic reticulum developed properly. This suggests that development in a protected environment relieves the evolutionary pressure in amniotes to develop the early motility that, in fish, is essential for escaping from predators. Obviously complex functions such as locomotion are likely to depend on numerous genes and their biochemical pathways related to muscle energy metabolism and calcium handling. On the basis of these considerations, we can speculate that zebrafish have developed different strategies from mammals for sarcoplasmic reticulum development.

Nevertheless, we demonstrate that the role of the zebrafish *nfixa* in regulating the proper switch towards the secondary myogenic wave is conserved during vertebrate evolution: its absence determines the persistent expression of primary slow MyHC when, naturally, their level should decrease. According to these data, we also observed an increased proliferation of primary muscle cells in *nfixa*-MO injected larvae at 3 dpf when normally in wild-type fish the significant slow fibers deposition occurs before 3 dpf (Barresi et al., 2001). This evolutionary Nfix conserved mechanism is also supported by evidence that indicates, as in mouse, the involvement of *Mef2* and *Nfatc4*. In fact, we have demonstrated that, in zebrafish, *Nfix2* acts only with its co-factors *Mef2a* and *Mef2c*, as the rescue happens only with the co-injection of all the transcripts together. Moreover as in mouse, *nfix*a negatively modulates the expression of *nfatc4* which, in turn, is responsible for the physiological expression of primary slow MyHC. In *nfixa* loss-of-function larvae, *nfatc4* transcript levels are increased, leading to a persistent expression of primary slow MyHC, whereas the downregulation of *nfatc4* restore normal primary slow MyHC levels in the *nfixa*-MO injected zebrafish embryos.

Moreover, we observed that the persistent expression of slow-MyHC in primary fibers following *nfixa* loss-of-function, causes the absence of the second myogenic wave. But at variance with mouse, we observed that the Pax7-positive precursors of secondary fibers at the external layers of the myotome are absent in *nfixa*-MO larvae at 3 dpf. These *pax7*-positive cells in zebrafish are similar to those found in amniotes, and participate in hypertrophic growth during larval stages, as well as in muscle repair after injury or in dystrophic conditions (Seger et al., 2011). In our previous work, we demonstrated that the expression of the murine *Pax7* does not depend on *Nfix* but rather is required for *Nfix* expression at the onset of the fetal myogenesis (Messina et al., 2010). The results we obtained in zebrafish might be explained with a feedback loop exerted by *nfixa* on *pax7* expression; alternatively, the action of *nfixa* on *pax7* expression might be indirect. Further experiments will be needed to elucidated this pathway.

Although an embryonic and fetal myogenesis in zebrafish have not been yet described in great detail, our experimental evidence provides a clue for comprehending the mechanisms that regulate this process. Previous work from several laboratories demonstrated the existence of mechanisms that specifically regulate the development of slow muscle in the early embryo. For example, the specification of some secondary slow fibers is independent of Hh signaling, which is rather essential for the development of primary slow fibers (Buckingham, 2007; Devoto et al., 1996). The *nfixa* involvement in the second myogenic wave correlates well with its expression peak at 48 hpf, because, during somitogenesis, *nfixa* knockdown does not alter the initial formation of slow muscle precursors in zebrafish embryos. Interestingly, the loss of function of other genes expressed during somitogenesis, such as *smyhc1*, also produces a phenotype only during the second myogenic wave (Codina et al., 2010).

In conclusion, our data suggest that, at least for this molecular pathway, the second myogenic wave in fish may correspond to fetal myogenesis in mammals through a mechanism that is mainly conserved. Indeed, we clearly demonstrate that the role of Nfix in driving the second myogenic wave and in the regulation of primary slow myosin embryonic fibers is strongly conserved during evolution. Unfortunately, our knowledge of morphological and biochemical differences between the primary and secondary myogenesis in fish is

still modest when compared with what already known in mammals. This prevents us from achieving an in depth understanding of the similarities and differences between these myogenic waves. Further work will hopefully address this issue in the future.

Acknowledgements
We thank S. Elworthy for the *smych1* construct, and P. Ingham for his priceless support, suggestions and for critical reading of the manuscript. We also thank U. Fascio, Miriam Ascagni, L. Ferrari, C. Brusegan, C. Bonfanti, C. Lora Lamia, A. Frassine, L. Del Giacco and A. Barbuti for their invaluable support.

Funding
This work was supported by grants from the EC FP7VII [223098] (Optistem), from the ERC StG 2011 [RegeneratioNfix 280611] and from the Italian Ministry of Research.

Competing interests statement
The authors declare no competing financial interests.

Supplementary material
Supplementary material available online at
http://dev.biologists.org/lookup/suppl/doi:10.1242/dev.076315/-/DC1

References

Amali, A. A., Lin, C. J., Chen, Y. H., Wang, W. L., Gong, H. Y., Lee, C. Y., Ko, Y. L., Lu, J. K., Her, G. M., Chen, T. T. et al. (2004). Up-regulation of muscle-specific transcription factors during embryonic somitogenesis of zebrafish (Danio rerio) by knock-down of myostatin-1. *Dev. Dyn.* **229**, 847-856.
Barresi, M. J., D'Angelo, J. A., Hernandez, L. P. and Devoto, S. H. (2001). Distinct mechanisms regulate slow-muscle development. *Curr. Boil.* **11**, 1432-1438.
Biressi, S., Molinaro, M. and Cossu, G. (2007). Cellular heterogeneity during vertebrate skeletal muscle development. *Dev. Biol.* **308**, 281-293.
Biressi, S., Messina, G., Collombat, P., Tagliafico, E., Monteverde, S., Benedetti, L., Cusella De Angelis, M. G., Mansouri, A., Ferrari, S., Tajbakhsh, S. et al. (2008). The homeobox gene Arx is a novel positive regulator of embryonic myogenesis. *Cell Death Differ.* **15**, 94-104.
Blagden, C. S., Currie, P. D., Ingham, P. W. and Hughes, S. M. (1997). Notochord induction of zebrafish slow muscle mediated by Sonic hedgehog. *Genes Dev.* **11**, 2163-2175.
Bryson-Richardson, R. J., Daggett, D. F., Cortes, F., Neyt, C., Keenan, D. G. and Currie, P. D. (2005). Myosin heavy chain expression in zebrafish and slow muscle composition. *Dev. Dyn.* **233**, 1018-1022.
Buckingham, M. (2007). Skeletal muscle progenitor cells and the role of Pax genes. *C. R. Biol.* **330**, 530-533.
Calabria, E., Ciciliot, S., Moretti, I., Garcia, M., Picard, A., Dyar, K. A., Pallafacchina, G., Tothova, J., Schiaffino, S. and Murgia, M. (2009). NFAT isoforms control activity-dependent muscle fiber type specification. *Proc. Natl. Acad. Sci. USA* **106**, 13335-13340.
Campbell, C. E., Piper, M., Plachez, C., Yeh, Y. T., Baizer, J. S., Osinski, J. M., Litwack, E. D., Richards, L. J. and Gronostajski, R. M. (2008). The transcription factor Nfix is essential for normal brain development. *BMC Dev. Biol.* **8**, 52.
Cermenati, S., Moleri, S., Cimbro, S., Corti, P., Del Giacco, L., Amodeo, R., Dejana, E., Koopman, P., Cotelli, F. and Beltrame, M. (2008). Sox18 and Sox7 play redundant roles in vascular development. *Blood* **111**, 2657-2666.
Chang, E. J. and Mun, K. C. (2004). Effect of melatonin on the malondialdehyde level of neutrophils in cyclosporine-treated rats. *Transplant. Proc.* **36**, 2165-2166.
Chen, J. K., Taipale, J., Cooper, M. K. and Beachy, P. A. (2002). Inhibition of Hedgehog signaling by direct binding of cyclopamine to Smoothened. *Genes Dev.* **16**, 2743-2748.
Chen, J. C., Mortimer, J., Marley, J. and Goldhamer, D. J. (2005). MyoD-cre transgenic mice: a model for conditional mutagenesis and lineage tracing of skeletal muscle. *Genesis* **41**, 116-121.
Codina, M., Li, J., Gutiérrez, J., Kao, J. P. and Du, S. J. (2010). Loss of Smyhc1 or Hsp90alpha1 function results in different effects on myofibril organization in skeletal muscles of zebrafish embryos. *PLoS ONE* **5**, e8416.
Cossu, G. and Biressi, S. (2005). Satellite cells, myoblasts and other occasional myogenic progenitors: possible origin, phenotypic features and role in muscle regeneration. *Semin. Cell Dev. Biol.* **16**, 623-631.
Coutelle, O., Blagden, C. S., Hampson, R., Halai, C., Rigby, P. W. and Hughes, S. M. (2001). Hedgehog signalling is required for maintenance of myf5 and myoD expression and timely terminal differentiation in zebrafish adaxial myogenesis. *Dev. Biol.* **236**, 136-150.
Del Giacco, L., Pistocchi, A. and Ghilardi, A. (2010). prox1b Activity is essential in zebrafish lymphangiogenesis. *PLoS ONE* **5**, e13170.
Devoto, S. H., Melançon, E., Eisen, J. S. and Westerfield, M. (1996). Identification of separate slow and fast muscle precursor cells in vivo, prior to somite formation. *Development* **122**, 3371-3380.
Driller, K., Pagenstecher, A., Uhl, M., Omran, H., Berlis, A., Gründer, A. and Sippel, A. E. (2007). Nuclear factor I X deficiency causes brain malformation and severe skeletal defects. *Mol. Cell. Biol.* **27**, 3855-3867.
Du, S. J., Devoto, S. H., Westerfield, M. and Moon, R. T. (1997). Positive and negative regulation of muscle cell identity by members of the hedgehog and TGF-beta gene families. *J. Cell Biol.* **139**, 145-156.
Elworthy, S., Hargrave, M., Knight, R., Mebus, K. and Ingham, P. W. (2008). Expression of multiple slow myosin heavy chain genes reveals a diversity of zebrafish slow twitch muscle fibres with differing requirements for Hedgehog and Prdm1 activity. *Development* **135**, 2115-2126.
Granato, M., van Eeden, F. J., Schach, U., Trowe, T., Brand, M., Furutani-Seiki, M., Haffter, P., Hammerschmidt, M., Heisenberg, C. P., Jiang, Y. J. et al. (1996). Genes controlling and mediating locomotion behavior of the zebrafish embryo and larva. *Development* **123**, 399-413.
Gros, J., Manceau, M., Thomé, V. and Marcelle, C. (2005). A common somitic origin for embryonic muscle progenitors and satellite cells. *Nature* **435**, 954-958.
Henry, C. A. and Amacher, S. L. (2004). Zebrafish slow muscle cell migration induces a wave of fast muscle morphogenesis. *Dev. Cell* **7**, 917-923.
Higashijima, S., Hotta, Y. and Okamoto, H. (2000). Visualization of cranial motor neurons in live transgenic zebrafish expressing green fluorescent protein under the control of the islet-1 promoter/enhancer. *J. Neurosci.* **20**, 206-218.
Hollway, G. E., Bryson-Richardson, R. J., Berger, S., Cole, N. J., Hall, T. E. and Currie, P. D. (2007). Whole-somite rotation generates muscle progenitor cell compartments in the developing zebrafish embryo. *Dev. Cell* **12**, 207-219.
Hutcheson, D. A., Zhao, J., Merrell, A., Haldar, M. and Kardon, G. (2009). Embryonic and fetal limb myogenic cells are derived from developmentally distinct progenitors and have different requirements for beta-catenin. *Genes Dev.* **23**, 997-1013.
Kimmel, C. B., Ballard, W. W., Kimmel, S. R., Ullmann, B. and Schilling, T. F. (1995). Stages of embryonic development of the zebrafish. *Dev. Dyn.* **203**, 253-310.
Messina, G., Biressi, S., Monteverde, S., Magli, A., Cassano, M., Perani, L., Roncaglia, E., Tagliafico, E., Starnes, L., Campbell, C. E. et al. (2010). Nfix regulates fetal-specific transcription in developing skeletal muscle. *Cell* **140**, 554-566.
Nasevicius, A. and Ekker, S. C. (2000). Effective targeted gene 'knockdown' in zebrafish. *Nat. Genet.* **26**, 216-220.
Panzer, J. A., Gibbs, S. M., Dosch, R., Wagner, D., Mullins, M. C., Granato, M. and Balice-Gordon, R. J. (2005). Neuromuscular synaptogenesis in wild-type and mutant zebrafish. *Dev. Biol.* **285**, 340-357.
Relaix, F., Rocancourt, D., Mansouri, A. and Buckingham, M. (2005). A Pax3/Pax7-dependent population of skeletal muscle progenitor cells. *Nature* **435**, 948-953.
Robu, M. E., Larson, J. D., Nasevicius, A., Beiraghi, S., Brenner, C., Farber, S. A. and Ekker, S. C. (2007). p53 activation by knockdown technologies. *PLoS Genet.* **3**, e78.
Schnapp, E., Pistocchi, A. S., Karampetsou, E., Foglia, E., Lamia, C. L., Cotelli, F. and Cossu, G. (2009). Induced early expression of mrf4 but not myog rescues myogenesis in the myod/myf5 double-morphant zebrafish embryo. *J. Cell Sci.* **122**, 481-488.
Seger, C., Hargrave, M., Wang, X., Chai, R. J., Elworthy, S. and Ingham, P. W. (2011) Analysis of Pax7 expressing myogenic cells in zebrafish muscle development, injury, and models of disease. *Dev. Dyn.* **240**, 2440-2451.
Steele-Perkins, G., Butz, K. G., Lyons, G. E., Zeichner-David, M., Kim, H. J., Cho, M. I. and Gronostajski, R. M. (2003). Essential role for NFI-C/CTF transcription-replication factor in tooth root development. *Mol. Cell. Biol.* **23**, 1075-1084.
Steele-Perkins, G., Plachez, C., Butz, K. G., Yang, G., Bachurski, C. J., Kinsman, S. L., Litwack, E. D., Richards, L. J. and Gronostajski, R. M. (2005). The transcription factor gene Nfib is essential for both lung maturation and brain development. *Mol. Cell. Biol.* **25**, 685-698.
Stellabotte, F., Dobbs-McAuliffe, B., Fernández, D. A., Feng, X. and Devoto, S. H. (2007). Dynamic somite cell rearrangements lead to distinct waves of myotome growth. *Development* **134**, 1253-1257.
Stickney, H. L., Barresi, M. J. and Devoto, S. H. (2000). Somite development in zebrafish. *Dev. Dyn.* **219**, 287-303.
Taylor, J. S., Braasch, I., Frickey, T., Meyer, A. and Van de Peer, Y. (2003). Genome duplication, a trait shared by 22000 species of ray-finned fish. *Genome Res.* **13**, 382-390.
Thisse, C., Thisse, B., Schilling, T. F. and Postlethwait, J. H. (1993). Structure of the zebrafish snail1 gene and its expression in wild-type, spadetail and no tail mutant embryos. *Development* **119**, 1203-1215.
Thompson, M. A., Ransom, D. G., Pratt, S. J., MacLennan, H., Kieran, M. W., Detrich, H. W., 3rd, Vail, B., Huber, T. L., Paw, B., Brownlie, A. J. et al. (1998). The cloche and spadetail genes differentially affect hematopoiesis and vasculogenesis. *Dev. Biol.* **197**, 248-269.
Weinberg, E. S., Allende, M. L., Kelly, C. S., Abdelhamid, A., Murakami, T., Andermann, P., Doerre, O. G., Grunwald, D. J. and Riggleman, B. (1996). Developmental regulation of zebrafish MyoD in wild-type, no tail and spadetail embryos. *Development* **122**, 271-280.

Fig. S1. Spatial expression of *nfixb* and *nfixa* analyzed by whole-mount in situ hybridization. (**A**) *nfixb*-specific probe has no signal in somitogenesis. (**B**,**C**) At 3 dpf the signals of both *nfixb* common probe and *nfixa* specific probe are detected in the central nervous system. t, telencephalon; m, mesencephalon. In all figures, lateral views are shown, anterior is always towards the left. Scale bar: 100 μm.

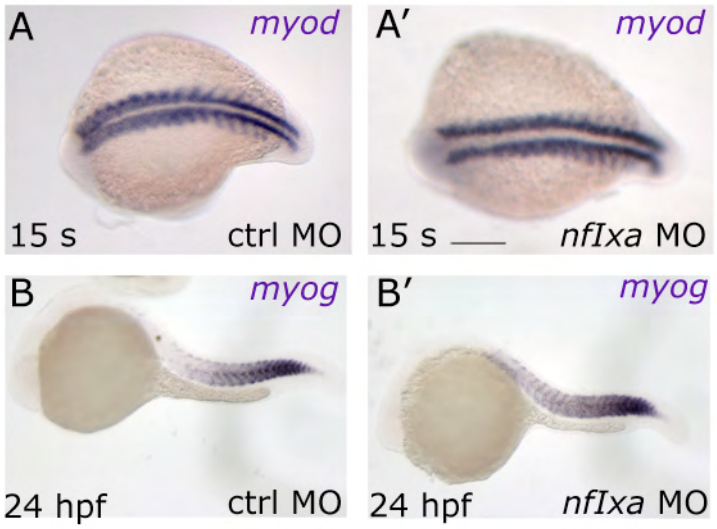

Fig. S2. First myogenic wave takes place correctly in *nfixa*-MO-injected embryos. (**A-B′**) *myod* (A,A′) and *myog* (B,B′) expression patterns in *nfixa*-MO embryos during somitogenesis and at 24 hpf are the same as control, suggesting that the segmentation process and the first myogenic wave are correctly formed. In A,A′, dorsal views are shown; in B,B′ lateral views are shown. Anterior is always towards the left. Scale bars: 100 μm in A,A′; 150 μm in B,B′.

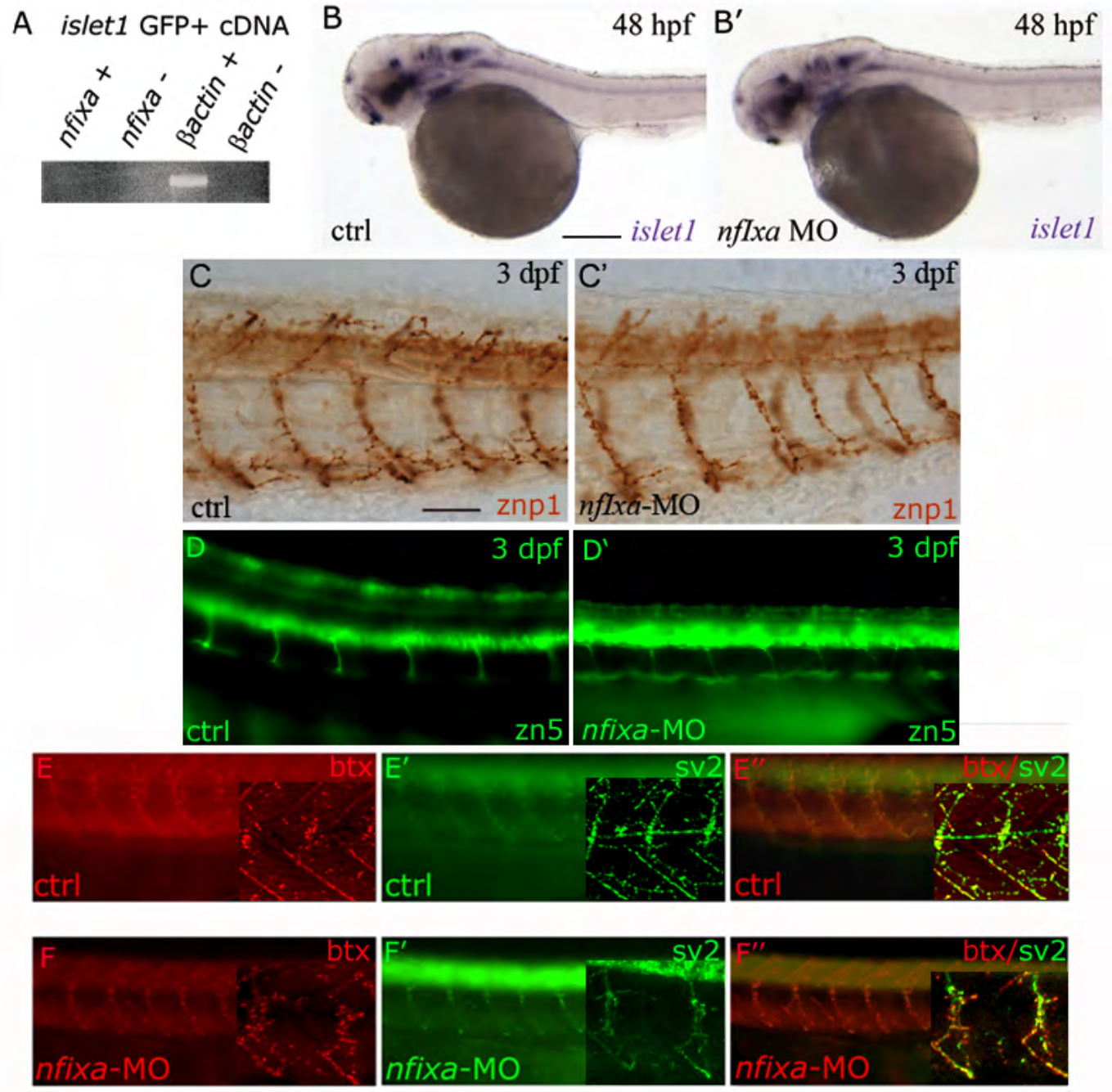

Fig. S3. ***Nfixa*** **loss of function does not influence motoneurons development** (**A**) RT-PCR performed on cDNA of motoneurons sorted from *islet1* GFP transgenic embryos at 48 hpf. *nfixa* is not expressed in this cell population. (**B**,**B′**) *islet1* expression pattern in *nfixa*-MO embryos at 48 hpf does not present differences in comparison with control embryos, suggesting that motoneurons are correctly formed. (**C-D′**) Axonal projections of primary (C,C′) and secondary motoneurons (D,D′) visualized by znp1 and zn-5 antibodies, respectively, are correctly formed in *nfixa*-MO-injected embryos. (**E-F″**) Synapses were labeled with bungarotoxin (BTX red, postsynaptic AChRs) and SV2 (green, presynaptic vesicles) antibodies. The co-localization of both signals in control (E″) and *nfixa*-MO injected (F′) embryos showed functional neuromuscular synapses. Main panels are images taken on a fluorescence microscope; insets show single-plane confocal images/projections from a confocal *z*-stack.

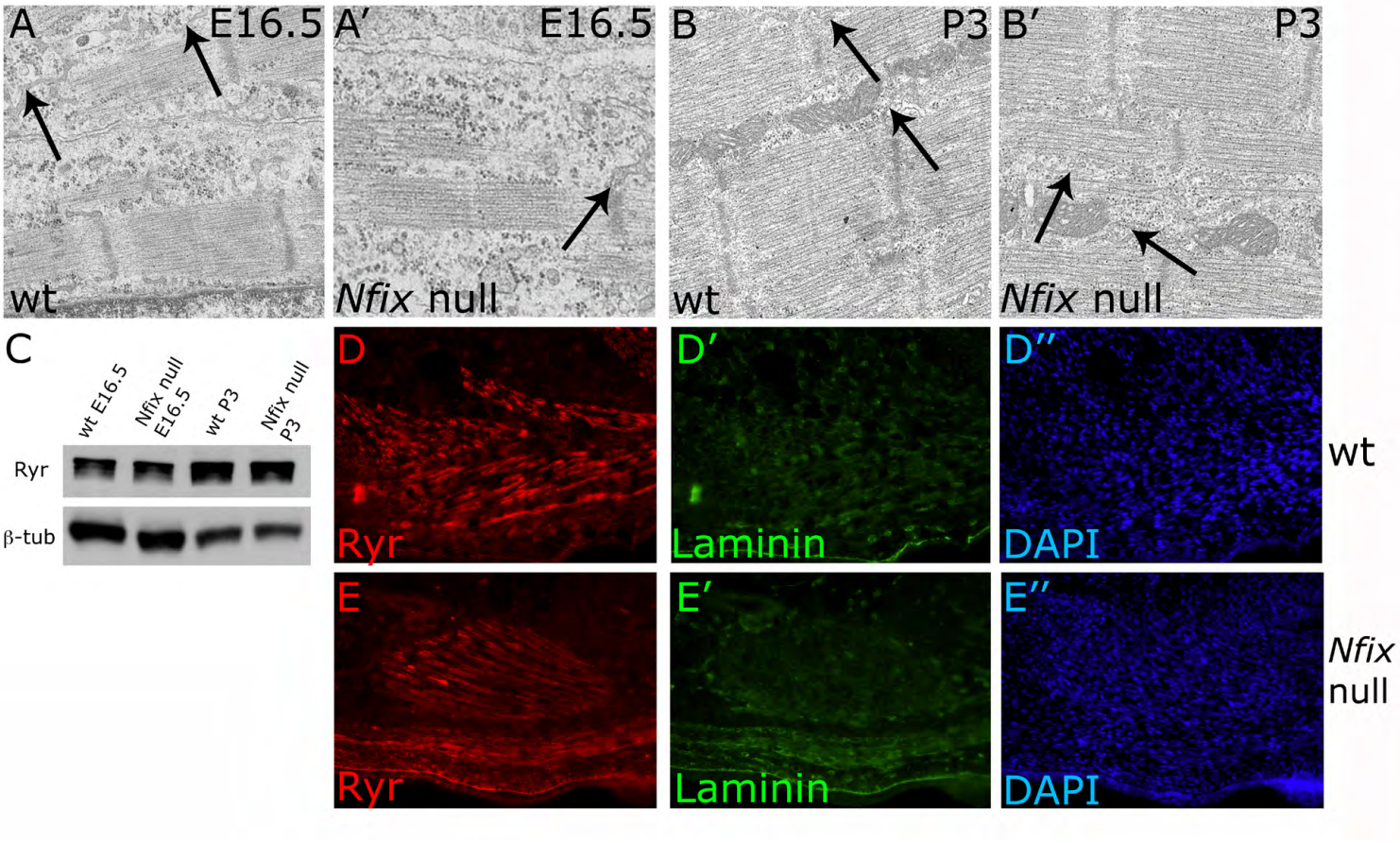

Fig. S4. Sarcoplasmic reticulum (SR) is correctly formed in skeletal muscle *Nfix*-null mice. (**A-E″**) Investigation of the SR phenotype both in specific skeletal muscle *Nfix*-null mouse (*Nfix*-null) fetal E16.5 and in postnatal P3 developmental stages by means of TEM (A-B′), Western blot analyses (C) and immunostaining for RyR (red, D,E). Laminin staining (green, D′,E′); DAPI staining (blue, D″,E″).

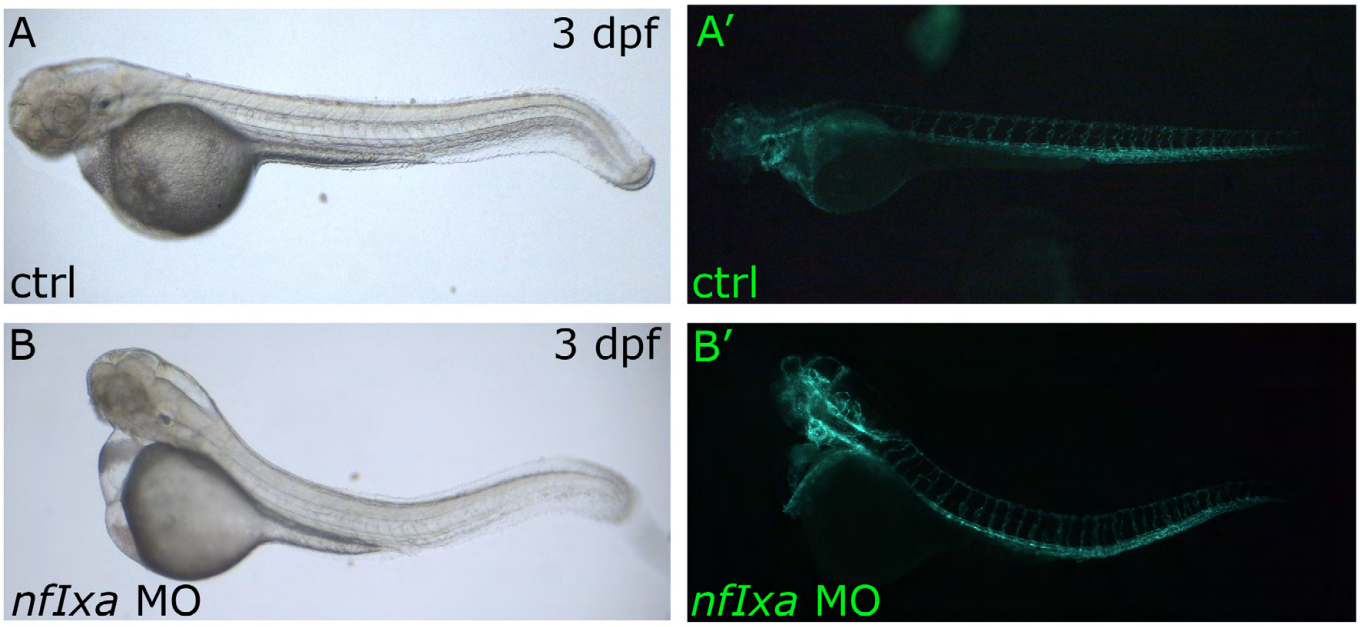

Fig. S5. Vessel formation is comparable in control and *nfixa*-MO *flil*-GFP-trangenic injected embryos. (**A-B′**) Visible (A,B) and fluorescent images (A′,B′) of GFP-vessels visualized in control (A,A′) and *nfixa*-MO (B,B′) injected embryos at 3 dpf.

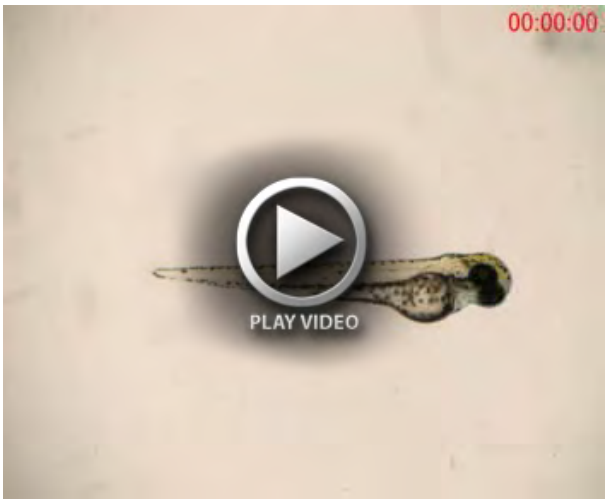

Movie 1. At 48 hpf, ctrl-MO embryos properly swim after stimuli. Embryos were tested with a tactile stimulus response assay.

Movie 2. At 48 hpf, *nfixa*-MO injected embryos present reduced touch-response. Embryos were tested with a tactile stimulus response assay. *nfixa*-MO injected embryos are less sensitive to tactile stimuli than ctrl-MO embryos and do not swim away when touched.

Movie 3. Partial rescue of *nfixa*-MO injected embryos by means of the murine *Nfix2* isoform mRNA injection together with its co-factors *Mef2a* and *Mef2c.* Embryos were tested with a tactile stimulus response assay. *nfixa*-MO (8 ng/embryo) was injected with murine isoform *Nfix2* (200 pg/embryo), *Mef2a* (150 pg/embryo) and *Mef2c* (150 pg/embryo) mRNAs. The immotile phenotype was partially rescued in 35% (*n*=70) of the injected embryos, i.e. they swam away (in a circle) when stimulated.

Table S1. Zebrafish Nfixa and Nfixb proteins are highly similar to the mammalian Nfix proteins

	Zebrafish nfixb		Human NFIX		Miuse Nfix	
	Identity	Similarity	Identity	Similarity	Identity	Similarity
Zebrafish Nfixa (542 amino acids)	87%	92%	81%	84%	76%	81%
Zebrafish Nfixb (556 amino acids)	--	--	81%	85%	81%	86%

Similarity and identity levels between human, mouse and zebrafish Nfix proteins reported were obtained with the program BLASTP (version 2.2.21+).